

Attaining stable electrolyzer operation under multi-annual climatic variations in almost fully renewable electricity systems: the case of Sweden

Christian Mikovits^a, Elisabeth Wetterlund^{b,c,*}, Sebastian Wehrle^a, Johann Baumgartner^a, Johannes Schmidt^a

^a*Institute for Sustainable Economic Development, University of Natural Resources and Life Science, Vienna, Austria*

^b*Energy Engineering, Division of Energy Science, Luleå University of Technology, 971 87 Luleå, Sweden*

^c*International Institute for Applied Systems Analysis (IIASA), A-2361 Laxenburg, Austria*

Abstract

Hydrogen produced from renewable electricity can play an important role in deep decarbonization of industry, such as primary steel-making. However, adding large electrolyzer capacities to a low-carbon electricity system also increases the need for additional renewable electricity generation which will mostly come from variable renewable energies (VRE). This will require hydrogen production to be variable, unless sufficient flexibility is provided by other sources. Existing sources of flexibility in hydro-thermal systems are (a) hydropower and (b) thermal generation. However, increasing the flexibility of hydropower generation may have negative consequences for river ecosystems and the use of fossil and non-fossil fuels in generation may increase if thermal power is increasingly used to balance short-falls in wind power during electrolyzer operation. We assess here for our Swedish case study the utilization of electrolyzers with a dispatch model, assuming that additional VRE generation matches the additional electricity demand of hydrogen production on average. The flexibility of hydropower and thermal generation is restricted in four scenarios, and we run our model for 29 different weather years to test the impact of variable weather regimes. We show that (a) in all scenarios, electrolyzer utilization is above 60% on average, (b) the inter-annual variability of hydrogen production is very high if thermal power is not dispatched for electrolysis, (c) this problem is aggravated if hydropower flexibility is also restricted, and therefore (d) either

*Corresponding author

Email addresses: christian.mikovits@boku.ac.at (Christian Mikovits), elisabeth.wetterlund@ltu.se (Elisabeth Wetterlund), sebastian.wehrle@boku.ac.at (Sebastian Wehrle), johann.baumgartner@boku.ac.at (Johann Baumgartner), johannes.schmidt@boku.ac.at (Johannes Schmidt)

long-term storage of hydrogen, backup hydrogen sources, or additional flexibility measures may be necessary to guarantee continuous hydrogen flows, and (e) adding wind power and electrolysis decreases the need for other backup flexibility measures in the system during climatic extreme events.

Keywords: renewables, hydrogen, flexibility, biomass, long-term analysis

1. Introduction

Hydrogen is considered as one important option for deep decarbonization of energy and industrial sectors, in particular in the fields of transportation [1], as feedstock for fuel or chemical production, as reductant in primary steel-making [2], or as energy storage in stationary heat and electricity applications [3–5]. Today, natural gas constitutes the primary source for hydrogen production [6]. However, to allow for an actual contribution to decarbonization, hydrogen has to be generated in a carbon-free way. The electrolysis of water, using carbon-free renewable electricity, is one potential technological pathway.

Significant additional amounts of renewable electricity generation have to come, however, from intermittent generation such as solar PV or wind power, i.e., variable renewable generation (VRE), at least in markets where hydropower potential is already used up to its full potential. In effect, variability of generation is set to increase in the absence of additional measures. Operating electrolyzers in a variable way to align with renewables' variability is possible in principle. Yet, due to their high investment cost, the economics of electrolyzers demand high utilisation rates, and 'peak shaving', i.e., using electrolyzers to produce hydrogen from limited peaks in intermittent generation, is therefore economically not competitive [7]. Also, the quantities of hydrogen produced would be relatively small if only otherwise curtailed electricity is used.

Attaining a high utilization rate of electrolyzers under high VRE penetration therefore may increase the need for other flexibility options in the system. Hydro-thermal systems, such as our Swedish case study system, offer already significant flexibility today as both hydropower with storage and thermal generation can adapt their output according to system demands.

Hydropower dominated systems can offer flexibility on all time scales, [8–11] from hours to seasons to years. The highly flexible operation of hydropower plants for system integration of VRE, however, causes increased rapid sub-daily fluctuations in water flow and water levels (hydropeaking). This conflicts with other environmental quality objectives as short-term river regime alteration poses

a key threat to river ecosystems [12–15]. The negative impacts of a higher penetration of renewables on hydropeaking have indeed been assessed before [16].

Using thermal power generation more flexibly has minor consequences in terms of a lower efficiency of thermal power plants in part load operation [17]. However, depending on the system setup, thermal generation may even increase if used to guarantee a high utilization rate for electrolyzers. This comes at the cost of increased usage of fuels and associated air pollution impacts [18] and CO₂-emissions. The increased use of biomass as an alternative to fossil fuels also has its own environmental risks [19] and is limited by the sustainable sourcing potential. Thermal power generation should therefore be limited.

The role of electrolysis-based hydrogen in energy and electricity systems has been widely investigated in previous work, and several recent reviews show the important role of hydrogen in a future decarbonized energy world [3, 4, 20]. In particular, electrolyzers have been shown to increase the share of renewables in power systems such as in Europe [21], a sub-region in Norway [22], California [23], and Japan [24]. Hydrogen storage has also been shown to mitigate the problem of hydro-peaking [25] and to lower the spilling of water in hydropower cascades [26]. In most studies, hydrogen is assumed to be operated on surplus renewable electricity [7, 27–29] and existing studies have typically focused on the potential use of hydrogen for system integration of intermittent renewables. A limited amount of studies have assessed the production profile of renewable hydrogen production for industrial purposes [30–32]. None of the studies, however, assessed how climatic variations impact the long-term variability of hydrogen output and how existing flexibility measures can be used to stabilize hydrogen generation.

We therefore assess here in how far a high utilization rate of electrolyzers can be guaranteed in an almost fully renewable electricity system if additional electricity for electrolysis comes on average only from VRE, in particular wind power. We study the case of Sweden and assess the effect of gradually restricting the flexibility of hydropower and thermal power generation on the utilization of electrolyzers.

We chose Sweden as a case to study, as the country is well positioned to take a lead in the production of low-carbon hydrogen. Sweden has a power system with a very low CO₂-emission footprint, and strong policies in place to support full decarbonization, including a goal of 100 % renewable electricity production by 2040 [33]. The above-mentioned trade-off between increased hydropower production to meet future needs in the energy system and reduced environmental

impact on rivers is evident in the Swedish system [34], and hydropeaking has been observed as both high and increasing in Nordic regulated rivers [13, 35]. Hydrogen is also being outlined as a potential key technology in the future Swedish energy system, both as a flexibility technology to balance a high VRE share in the power system, for production of biofuels, and as reductant in the steel industry, where hydrogen is currently considered as the main track for decarbonization of primary steel-making [36–38]. While the results of our case study cannot be directly transferred, our conclusions do well apply also to other hydro-thermal systems with hydropower shares larger than 35% such as Brazil, Canada, New Zealand, or Austria [39].

Hydropower dominated electricity systems are prone to large inter-annual variations in water availability [40, 41]. To a limited extent, wind power systems also show inter-annual variability [41, 42]. A multi-year approach to assessing energy systems with high shares of renewables is therefore necessary [43]. In order to be able to realistically capture inter-annual variations and extreme weather events, we use simulations of time series of VRE and electricity demand in a dispatch model for the Swedish power system for 29 different weather years, at hourly temporal resolution. We can thus assess how both short-term (hours to days) and long-term (days to months to years) variability of climatic variables drive power production patterns. The model was developed by Höltinger et al. [41] and is extended to allow simulation of electrolyzer technology and a more detailed representation of thermal power generation and hydropower operational restrictions.

2. Material and methods

We assess here how different scenarios of thermal and hydropower flexibility affect the utilization of electrolyzers using a generation dispatch model for our case study of Sweden. In the following section, we present the general model structure and most relevant parts, as well as the major changes compared to the work by Höltinger et al. [41], with a more comprehensive and detailed model description given in Appendix A.1. The optimization program (written in *GAMS* and controlled by *Python*), the data necessary to run the simulations, the result of the simulations, and the *R* Code for result analysis can be found on Zenodo [44].

2.1. Dispatch model and data

2.1.1. Model description

The optimization model is based on hourly data for natural river runoff, load, and wind generation and aims to minimize total variable system cost less the revenue from hydrogen production. Residual demand, i.e., the mismatch of wind power generation and load, has to be balanced by thermal and hydropower plants, and curtailment of wind power. Potential further balancing needs are provided from further backup measures. These backup measures were assumed to be available at very low investment but high variable costs, as they are used with low frequency. Potential candidate technologies are additional thermal peaking plants, demand side management measures, or imports from neighboring countries. These are, however, not modelled in detail.

To be able to account for climate variability, the model was run for 29 different weather years, which were used to simulate *temperature dependent load*, *hydropower*, and *wind power* generation in the model. The model optimizes a single year of dispatch, i.e. inter-annual water storage was not considered.

A temperature dependent load profile of electricity demand was derived from a regression model based on reanalysis temperature data for 29 years and gridded population raster data (for details, see Höltinger et al. [41]). The modelled annual load is on average equal to the average annual observed load in the period 2010 - 2018 (approximately 130 TWh a^{-1} , excluding transmission losses). In addition, we have considered increased power demand from electrolysis (see section 2.2.1), but not from other uses such as increased demand by industry, data-centers, or from electrification of transportation.

Table 1 summarizes the characteristics of the included power plant types and other model components.

2.1.2. Wind power

For wind power, we used time series for potential future wind power production in Sweden, as modelled by Olauson et al. [45, 46]. The authors generated a range of different production scenarios, based on bias corrected wind speed data for Sweden. The assumed expansion of wind power is based on the assumption that nuclear power production is fully phased out and replaced by wind power, i.e. 60-65 TWh a^{-1} from 8.6 GW of installed capacity [47]. We also assumed a reduction of power exports to zero, which compares to observed net exports in the range of around 7.2 and 23 TWh a^{-1}

Table 1: Costs and capacities used. (CHP = combined heat and power, RDF = refuse derived fuel, NG = natural gas, NGCC = natural gas combined cycle, FST = condensing steam turbine, OCGT = open cycle gas turbine, IC = internal combustion engine, S = small, M = medium, L = large, I = industrial.)

	Production type	Fuel type	Installed capacity (MW)	Costs (€MWh ⁻¹)
Thermal Plants	Waste (CHP)	Waste	315	-63.2
	RDF (CHP)	Waste	385	5.55
	Biomass I (CHP)	Biomass	1,255	18.8
	Biomass L (CHP) ^a	Biomass	1,318	21.0
	Biomass M (CHP)	Biomass	603	24.8
	Biomass S (CHP)	Biomass	401	30.9
	NGCC L (CHP)	NG	701	57.9
	NGCC M (CHP)	NG	54	74.1
	NG IC (CHP)	NG	13	83.4
	FST	Oil & NG	905	125
	OCGT	Oil	1,579	152
	Biogas IC (CHP)	Biogas	21	156
	Hydropower	-	16,200	1
	Wind	-	varying ^b	0
	Additional backup measures	-	-	1,500
	Electrolysis	-	varying ^b	varying

^a This category also contains CHP plants currently using coal or peat as fuel (total installed capacity of 298 MW), as those were assumed to have been replaced by biomass CHP.

^b Wind and electrolysis capacity are directly coupled, detailed explanation in section 2.2.1

during the years 2011-2018 [47]. Further, we accounted for minimum thermal production from CHP plants (see section 2.1.4). This gives a total average annual wind power production of $49 \text{ TWh } a^{-1}$ from 14 GW of installed capacity, in the base scenario without hydrogen production. This compares to the current annual production of $17 \text{ TWh } a^{-1}$ from 7.4 GW of installed capacity (in 2018) [47]. The higher utilization of additional wind power can be partly attributed the addition of offshore wind capacities, and partly to larger rotor sizes.

In the modelled electrolysis scenarios, wind generation was scaled to match the increased electricity demand from electrolyzers, as described in section 2.2.1.

2.1.3. Hydropower

We followed the model formulation given in Höltinger et al. [41], which assumed a simplified hydropower model aggregating all hydropower plants to one reservoir and one plant. Simulated time series for river discharge from the hydrological catchment model S-HYPE were used [48, 49] and translated into power generation with a simulation model that takes the characteristics of all Swedish hydropower plants into account. A total reservoir capacity of 33.7 TWh was modelled, which needs to be kept between minimum (5%) and maximum (98%) observed levels during all hours [41, 50].

The reservoir level at the start of each year, as well as the required minimum level at the end of the year, were both set to 62%, which corresponds to the average reservoir filling level for the time period of 1960 to 2016 [50]. This represents a rather conservative approach which limits the possibility for hydropower to act as inter-annual storage, as extreme weather years with, e.g., low production of both hydro and wind power, cannot be dealt with by running down the levels of hydropower reservoirs at the end of the year. Historically, end-of-year reservoir levels have seen variations between 43% and 86% [50].

Hydropower operational limits, i.e., minimum flows and maximum ramping rates, were then assessed in two different scenarios (see section 2.2.3).

2.1.4. Thermal power generation

Höltinger et al. [41] did not differentiate between plant and fuel types; instead, thermal power generation was defined as one plant. We have here improved the original thermal generation model by disaggregating it into different plant technologies and fuel types.

Data on existing thermal power generation was compiled from the World Electric Power Plants database [51], and complemented by national statistics [52, 53]. Thermal production was categorised based on fuel, production scale and production technology, with each plant type defined by individual marginal generation cost and capacity (Table 1). Power production costs were based on projections for technology efficiency and fuel costs. Production costs further include a CO₂-charge (50 €/ton_{CO₂}), operation and maintenance cost, and heat credits, where applicable. Appendix A.2 provides the details on assumed cost and plant efficiencies.

Additionally, we have defined must-run conditions for different seasons of the year, as many plants serve heat demand from the residential and industry sectors. Generation in CHP plant was assumed to follow a monthly pattern throughout each year, with higher minimum production during the winter months, and lower minimum production during the summer. Additionally, maximum production was restricted during the summer period to account for maintenance and limited operation of CHP plants due to heat load restrictions. Annual production profiles were developed based on statistics of installed capacity and annual production per fuel type, in district heating systems and industrial back-pressure systems, respectively [50]. Expected annual full-load hour equivalents amount to 7500 h a⁻¹ for industrial biomass CHP and waste CHP, and 5000 h a⁻¹ for biomass CHP plants [54]. The load profiles applied in the optimization model are shown in Figure 1.

Maximum combined hourly ramping rates for the sum of thermal power generation were derived from historical observations of maximum ramping rates, and therefore set to 1.5 GW.

2.1.5. Hydrogen production

We have assumed that electrolyzer technology will advance beyond the current state-of-the-art (alkaline electrolysis), to proton exchange membranes (PEM). This has been reflected in our assumptions on hydrogen production efficiency, which was set to 72% (system efficiency, defined as hydrogen output on LHV basis divided by electrical input to the electrolysis system), corresponding to 46 kWh of electricity per kg hydrogen [55–57]. The electrolyzer was sized according to an expected electrolyzer utilization of 90%. As described in section 2.2.1, the utilization of the electrolyzer is actually a model output, which means that hydrogen demand in the different scenarios will not always be exactly met.

As PEM electrolyzers in general are highly flexible, with start-up times and ramping in the range of minutes or even seconds and very low minimum part-load operation (<10%), neither ramping

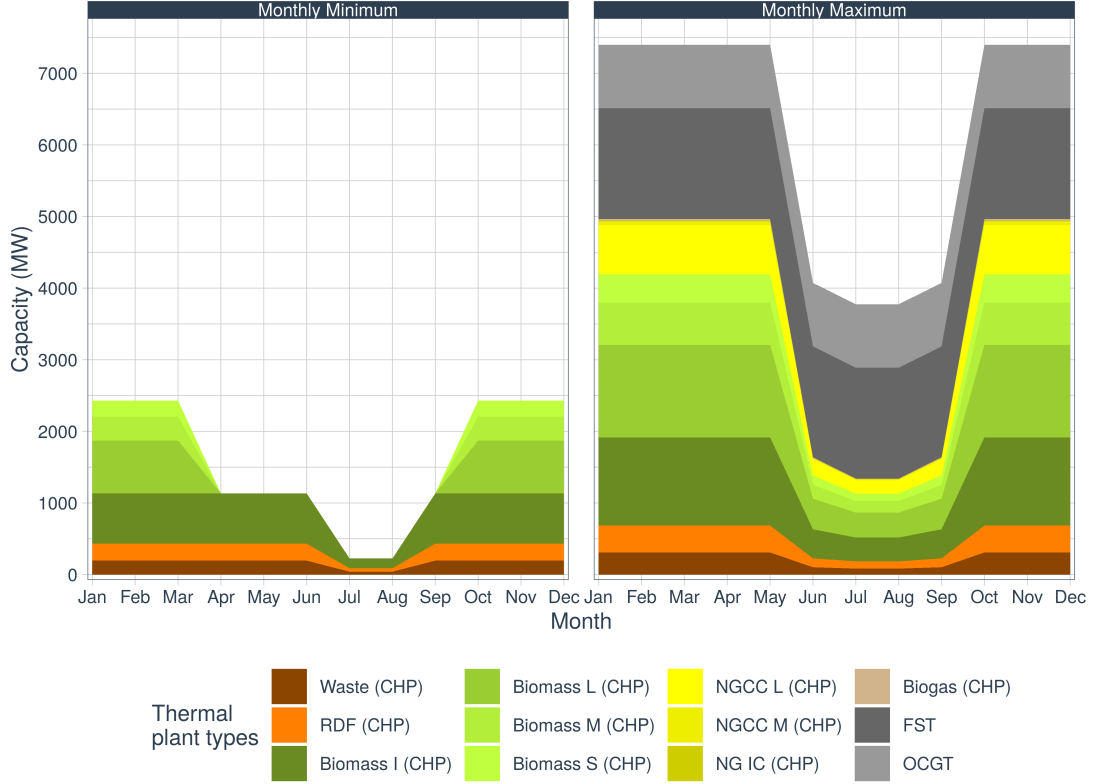


Figure 1: Modelled maximum (left) and minimum (right) thermal power production, per category. CHP = combined heat and power, RDF = refuse derived fuel, NG = natural gas, NGCC = natural gas combined cycle, FST = condensing steam turbine, OCGT = open cycle gas turbine, IC = internal combustion engine, S = small, M = medium, L = large, I = industrial.

nor electrolyzer part-load restrictions were considered in the model [57].

2.2. Scenarios

We defined increasing levels of demand for hydrogen (4 scenarios) and tested these demand scenarios under gradually more restricted flexibility in the system. First, we restricted thermal generation for hydrogen production by either allowing or not allowing the dispatch of thermal power generation for hydrogen production. Subsequently, we restricted the hydropower flexibility by limiting ramping and minimum river flows in two scenarios. This results in a total of 12 scenarios with hydrogen production plus two baseline scenarios without hydrogen demand (and therefore no

thermal dispatch for hydrogen scenario). Additionally, we ran a sensitivity analysis on the model for a wider set of hydrogen demands (see section 2.2.1).

2.2.1. Hydrogen demand

The hydrogen production scenarios were chosen so that they are able to deliver different amounts of hydrogen in order to satisfy different levels of future projected demand. We limited the hydrogen usage options to two pathways that are currently under development in Sweden: for hydrotreatment of different bio-based feedstocks in biofuel production, and as use as reductant in fossil-free primary steel-making according to the HYBRIT (Hydrogen Breakthrough Ironmaking Technology) route. We applied four different hydrogen scenarios, where one is the baseline scenario without electrolysis-based hydrogen (**NO**), and the other three (**SMALL**, **MEDIUM**, **LARGE**) can be considered as representing either different ambition levels for decarbonization, or different time perspectives. This results in different electrolysis loads on the system, as outlined in Table 2.

Table 2: Modelled hydrogen demand scenarios.

Scenario	Hydrogen for biofuels (TWh a^{-1})	Hydrogen for steel-making (TWh a^{-1})	Electrolyzer capacity (MW)
NO	0	0	0
SMALL	5	0	880
MEDIUM	10	0	1760
LARGE	10	10	3610

The estimates regarding biofuel production build on the ambitions announced by Preem, Sweden’s largest fuel producer, who has a goal of producing 3 million m^3 of biofuels by 2030 in their two refineries in Sweden [58]. Judging from their announced projects and plans, all biofuels will be drop-in fuels produced via hydroprocessing of various bio-crudes. Hydrogen is currently produced from refinery off-gases or via steam reforming of natural gas, but Preem has also expressed strong interest in hydrogen produced via electrolysis [58]. We have based our scenarios on the assumption that electrolysis-based hydrogen will be the main pathway in the future, and implemented two different annual demand levels; 5 and 10 TWh a^{-1} hydrogen, respectively. The lower level represents a scenario in which a large share of the biofuel feedstock has a relatively low oxygen content (e.g.,

used cooking oils or bio-crudes produced via hydrothermal liquefaction), while the higher scenario assumes a large share of biofuel feedstock with a higher oxygen content (e.g., lignin oil or fast pyrolysis oil) [59, 60].

In the **LARGE** scenario, we also assumed that the HYBRIT route will be fully implemented in Sweden, and that all primary steel-making via the blast furnace-basic oxygen furnace route will thus be replaced with hydrogen based direct reduction followed by electric arc furnaces. We only considered the projected additional electricity demand to cover the required hydrogen production ($10 \text{ TWh } a^{-1}$) [38, 61], while the additional electricity demand from downstream processes was excluded, similar to other industrial electrification (see section 2.1.1).

The scenarios were implemented by changing the restriction on electrolyzer capacity and scaling wind power in a way that on annual average, wind power generates enough electricity to supply the electrolyzer at full load. For instance, in an 880 MW electrolyzer scenario, we added wind capacity which on average generates $880 \times 8760 \text{ MWh } a^{-1}$. Thus, we can assess in how far the wind resource can be used for electrolysis and how much of the wind power is curtailed. Electrolyzer utilization is thus an output of the model, which means that the total defined hydrogen demand may not be exactly met in all scenarios, if it is too costly to do so.

In addition to the scenarios based on actual announced plans by different industrial actors, we applied a sensitivity analysis, where we tested extended capacities of electrolyzers - and associated increases in wind power generation - on a wide range of scenarios (5000 MW to 100,000 MW).

2.2.2. Thermal power flexibility

Additionally to varying the hydrogen demand, we also assessed the impact of dispatching thermal power plant for hydrogen production. Technically, we did so by varying the value of hydrogen in the objective function so that it was either below most (18 € MWh^{-1}) or above all (160 € MWh^{-1}) marginal costs of thermal generation. Thus, thermal power was either never or always dispatched to produce hydrogen. This represents two extreme settings, for which reason the results cover a wide range of possible outcomes. We refer to these scenarios as **NO THERMAL** and **THERMAL**, respectively.

2.2.3. Hydropower flexibility

We assessed two different scenarios regarding the impact of seasonal ramping restrictions and seasonal flow thresholds in the hydropower system, that represent two different hydropower regulation development pathways. The first scenario allows for high flexibility in the hydropower

operation, including the possibility for rapid flow fluctuations (**HI HYDRO FLEX**). The second scenario represents a more cautious scenario designed to prevent adverse impacts on river ecosystems from hydropeaking and water retention throughout low flow seasons (**LO HYDRO FLEX**). The restrictions were implemented by limiting the maximum ramping rate (MRR) and minimum flow (MF), following the approach proposed by Olivares et al.[62]. The **LO HYDRO FLEX** scenario is characterized by a very restrictive minimum flow rate of 50% and a maximum ramping rate of only 6% of median natural flow. In the **HI HYDRO FLEX** scenario, minimum flow is restricted to 20% and maximum ramping to 28% of median natural flow.

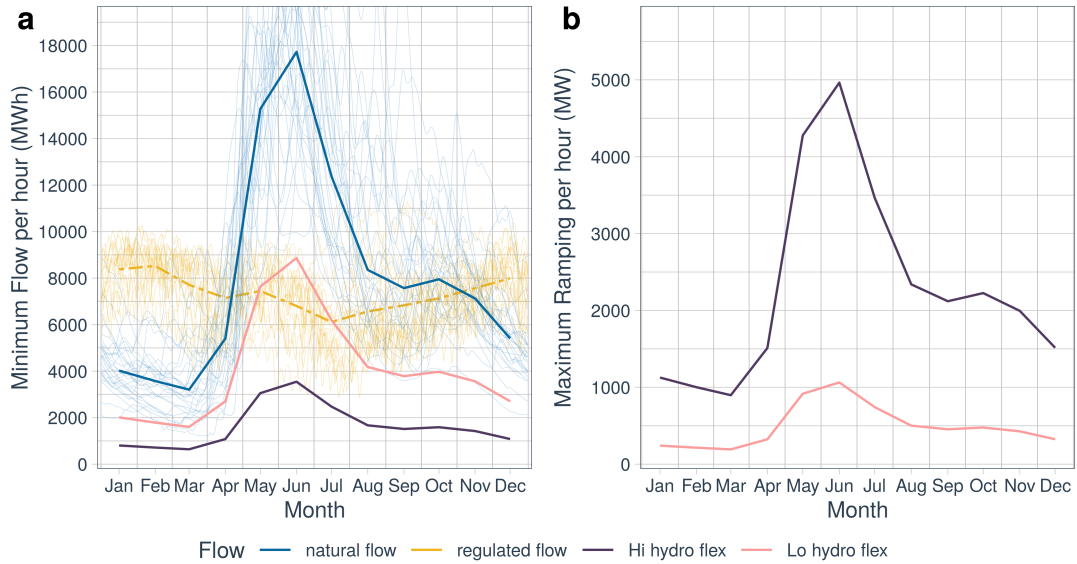


Figure 2: *a*: Minimum flow per hour (expressed as MWh h^{-1}), and *b*: Maximum allowed ramping per hour (expressed as MW h^{-1}), for the two modelled flexibility scenarios. *a* also shows the daily mean flows of all 29 weather years: natural and regulated.

The resulting monthly limits are displayed in figure 2, where *a* shows the minimum flow, and *b* the maximum ramping rates. These limits were derived from the simulation of potential natural flows (i.e., without human intervention) from the S-HYPE model [48, 49]. We observe the highest monthly median flow in June at about 18,000 MW, and the lowest flow in March, at only 3600 MW, which leads to a high variation throughout the year of both minimum flows and maximum ramping rates. Figure 2 *a* also shows the historical daily mean flows of all the 29 modelled weather years (blue) and the daily mean of 16 modelled weather years with regulated (human interference) flow

(yellow).

2.3. Model runs and performance indicators

We ran the optimization model for all scenarios outlined in the previous sections. Each scenario was evaluated for the 29 different weather years, at hourly temporal resolution. Our evaluation focused on the following performance indicators:

- Utilisation of electrolyzers (% of 8,760 hours)
- Inter-annual variability of hydrogen production (variance in utilisation across years)
- Thermal power generation ($\text{MWh } a^{-1}$)
- Required additional backup capacity (MW)
- Required additional backup energy ($\text{MWh } a^{-1}$)
- Variability in hydro flow (maximum hourly ramping) (MW)
- Minimum hydro flow (MW)

3. Results

The results focus on the utilization of electrolyzers, thermal generation, backup generation and capacity, and the changes in flows and minimum flows as induced by hydropower operation. The results of the base scenario without electrolyzer operation are shown where applicable.

3.1. Electrolyzer utilization

We first discuss here the electrolyzer utilization in the different scenarios. Figure 3 shows the annual utilization rate in all 29 simulated years for all scenarios. The average utilization rate is significantly lower for those scenarios which do not allow for the dispatch of thermal generation for hydrogen production. Additionally, lower hydropower flexibility decreases the utilization rate. For the `NO THERMAL` scenarios with high hydropower flexibility, the average utilization rate is mainly lowered by some extreme years, as can be observed from the difference between the median and the mean of the distribution. The average utilization rate of the electrolyzer increases with higher electrolyzer and wind power capacities in the `NO THERMAL` scenarios, while it decreases slightly

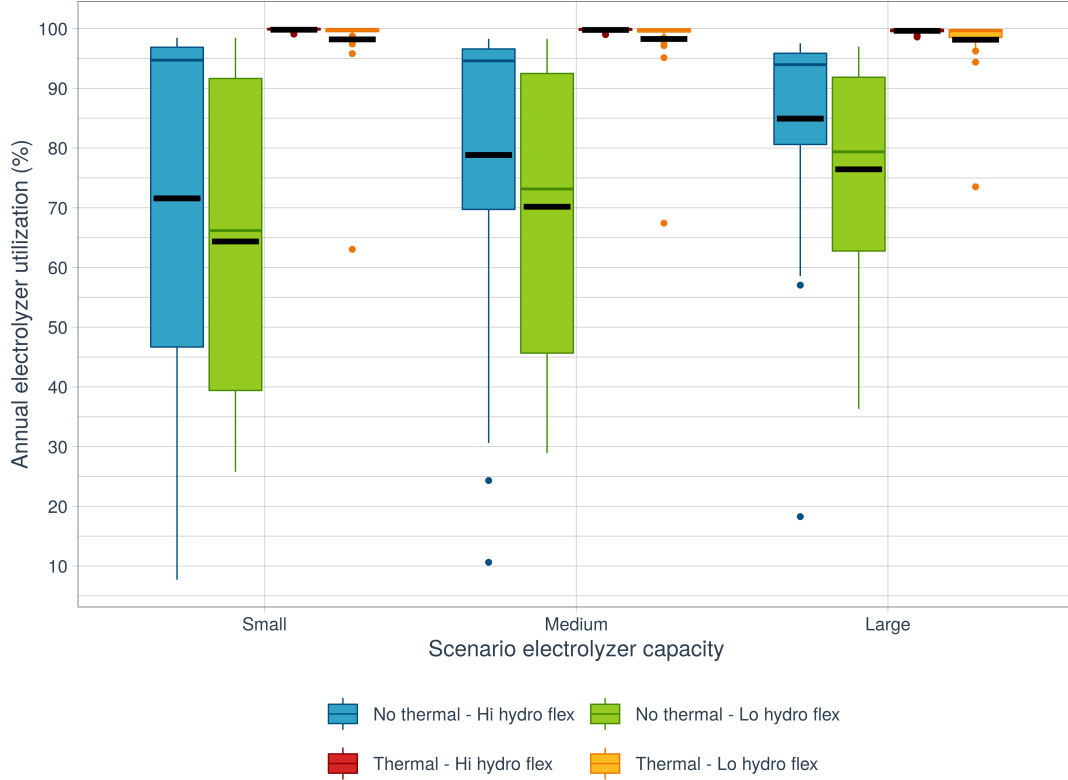


Figure 3: Boxplots of annual electrolyzer utilization in all scenarios. The black lines show the mean over all years.

for the **THERMAL** scenarios. The reason is that in the **NO THERMAL** scenarios, first wind power substitutes thermal power generation compared to the baseline scenario, as this reduces operational cost. However, this substitution effect is limited by the required minimum generation of thermal power production, as implied by heat demand. At higher electrolyzer and wind capacities, this causes an increase of excess wind power to use in hydrogen production. This effect is explored in more detail in section 3.5. The inter-annual variability of hydrogen production is very high for the **NO THERMAL** scenarios and the electrolyzer utilization drops to even below 25% for single years. This inter-annual variability is mainly driven by the variability in the availability of hydropower, and less so by variability in wind power generation or temperature dependent demand (see figure 4). This implies that single bad hydropower years have to be accounted for in the long-term planning of hydrogen supply, in case that the dispatch of thermal capacities for hydrogen production should

be prevented.

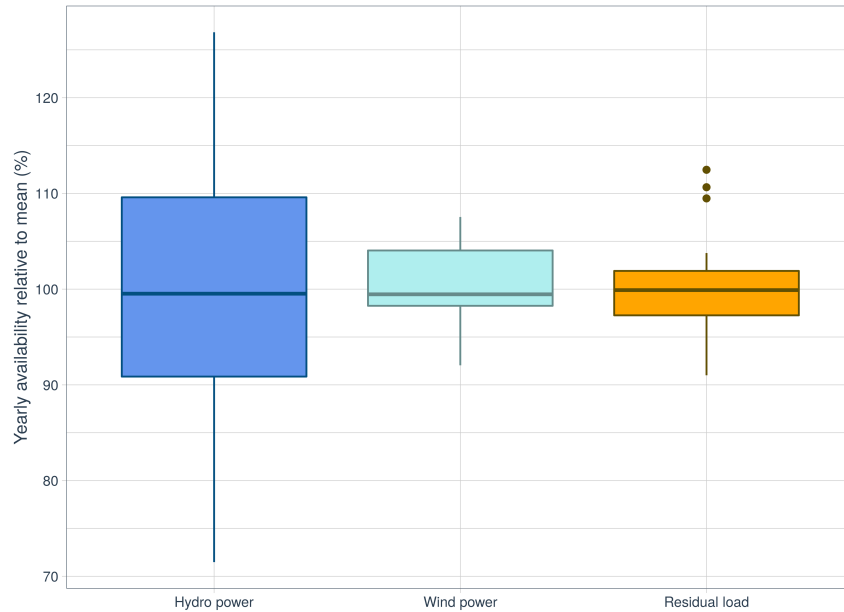


Figure 4: Annual variability of natural availability of hydropower, wind power, and temperature dependent residual load.

3.2. Thermal generation

The dispatch of thermal capacities in all scenarios is shown in figure 5. As could be expected, thermal generation is lower in the **NO THERMAL** scenarios, with the obvious exception of the **NO hydrogen capacity** scenario. Thermal generation is, correspondingly, higher for the **LO HYDRO FLEX** scenarios. Limiting hydropower flexibility increases the annual thermal power generation, on average, by 3 TWh in the **NO** scenario. It can be observed that for those scenarios, where thermal generation is not dispatched for electrolyzer operation, the total thermal generation even falls because additional wind power capacity is added to the system. This is, conversely, not the case for the **THERMAL** scenarios, where thermal generation is not replaced by additional wind power.

In the **LARGE** scenario, the difference in annual thermal generation increases to on average 8 TWh when comparing the two most extreme scenarios, i.e., the **NO THERMAL - HI HYDRO FLEX** and the **THERMAL - LO HYDRO FLEX** scenarios. In single years, this difference can amount to up to

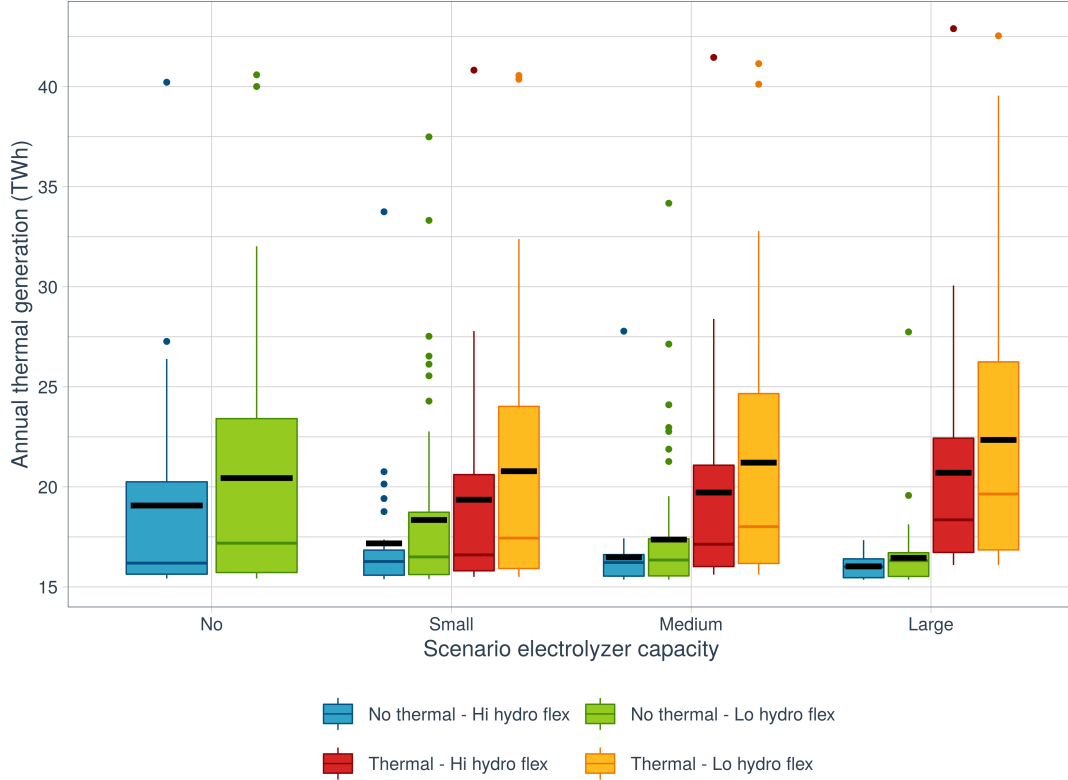


Figure 5: Annual thermal generation in all scenarios. Black lines show the mean over all years.

20 TWh. Again, this shows that while thermal power production is not essential to achieve sufficient electrolyzer utilization on average, in single years the dispatch of thermal power for electrolyzer operation will allow for significantly higher full load hours.

The share of thermal generation in total generation is between 11% and 17%, depending on the scenario. This, however, is mostly due to must-run conditions of thermal power plants, which have to generate at least 15 TWh of power to provide sufficient heat to heat consumers. Of course, in future systems with lower heat consumption and other heat sources, thermal generation may be reduced further.

Appendix A.3 shows details on how different thermal plant types are dispatched.

3.3. Backup generation and capacity

Backup generation and capacity is very low in all scenarios. If one extreme weather year, i.e. 1996, is removed from the data set, annual backup energy utilization is lower than 82 GWh in all remaining years (see figure 7), with a required annual backup capacity lower than 4 GW in all scenarios (see figure 6). Both the backup energy and the capacity fall with increasing electrolyzer capacity and corresponding wind power generation in the system, as electrolyzers are ramped down in hours when backup operation would otherwise be necessary. Electrolyzers, in tandem with the additional VRE generation capacities required to fuel them, can therefore provide crucial value to the system by reducing the amount of backup capacity necessary. In the **LARGE** scenario, backup capacity requirements fall to less than 2.5 GW. The difference between the hydropower flexibility scenarios is very low. Lower hydropower flexibility increases backup capacity and energy, but mostly due to one extreme year.

All scenarios run on at least 83% of wind and hydropower and only existing thermal generation capacities excluding nuclear are considered. The resulting backup requirements are low, and in particular the energy provided by those backup capacities is negligible, even if high variable costs are assumed. Providing, in total, on average 0.080 TWh of annual backup in the form of, e.g., demand response in a system that has a total demand of at least 130 TWh seems to be on a realistic scale.

3.4. Hydropower ramping and minimum flows

The distribution of hourly river flows and ramps in the system are shown in figure 8 for the **NO** and **LARGE** scenario. In Appendix A.4 all scenarios are shown in detail. The figure shows that the flexibility restrictions work as expected: ramps are lower and minimum flows are higher in the more restricted hydropower scenario. In particular, the spread of the distribution of flows in the more restricted scenario is narrower. Likewise, ramping is much more limited and also lower on average. Higher electrolyzer capacities slightly increase the spread in the river flows and in the magnitude of ramping events. Hydropower is therefore operated slightly more flexibly with increasing hydrogen production and added wind power capacity, as increased system variability is partly balanced by hydropower. There is almost no difference between the **NO THERMAL** and **THERMAL** scenarios if the same hydropower flexibility rules are applied, i.e., using thermal generation for hydrogen production does not affect the extreme conditions of hydropower operation.

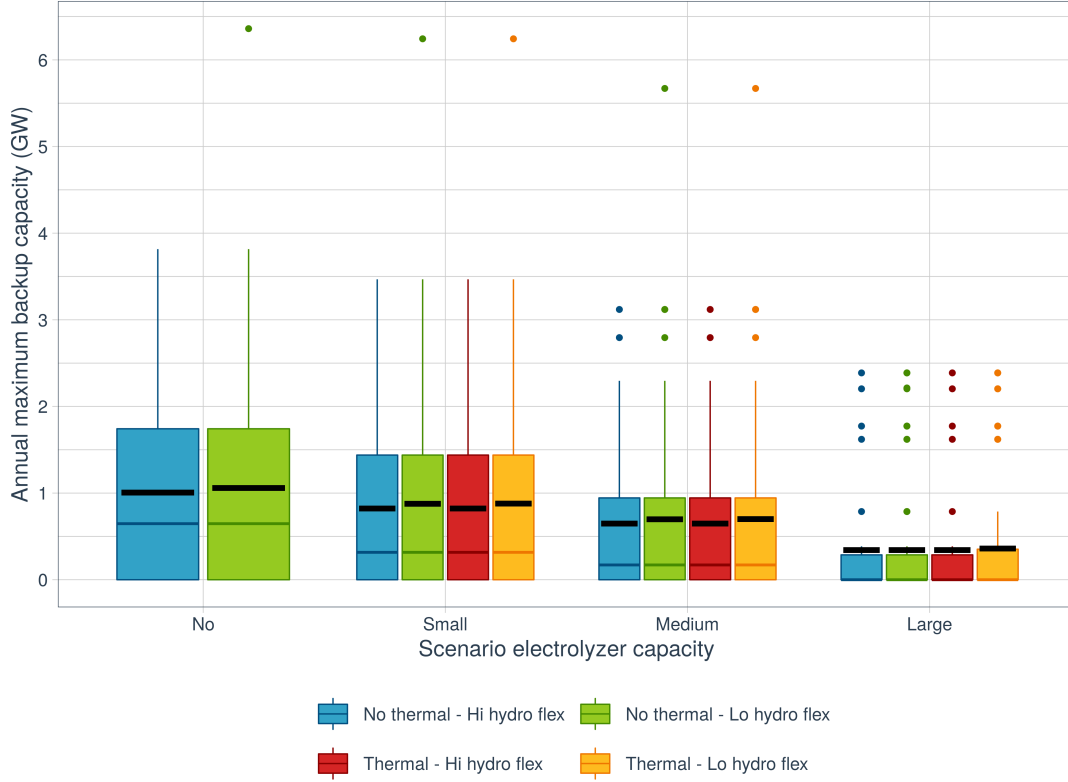


Figure 6: Annual required backup capacity in all scenarios. Black lines show the mean over all years.

Interestingly, extreme ramping events are, although allowed, rare. The maximum ramping allowed in the scenario with low flexibility is just above 1 GW. However, this ramping capacity is required at most in 0.3% of all hours in all scenarios, while ramping above 0.75 GW is only necessary in at most 1.9% of all hours. Likewise, a ramping capacity above 2 GW is only required in at most 0.4% of all hours in the scenario with high hydropower flexibility, where around 5 GW of ramping is allowed. This indicates that rapid ramping of hydropower is beneficial to the system in some moments, but is not massively required to balance the system.

3.5. Sensitivity analysis

Figure 9 shows the resulting utilization of electrolyzers when extending the capacities to very high levels, also including a corresponding expansion of wind power capacity.

The figure shows that an increase of the electrolyzer capacity up to around 8 GW of capacity

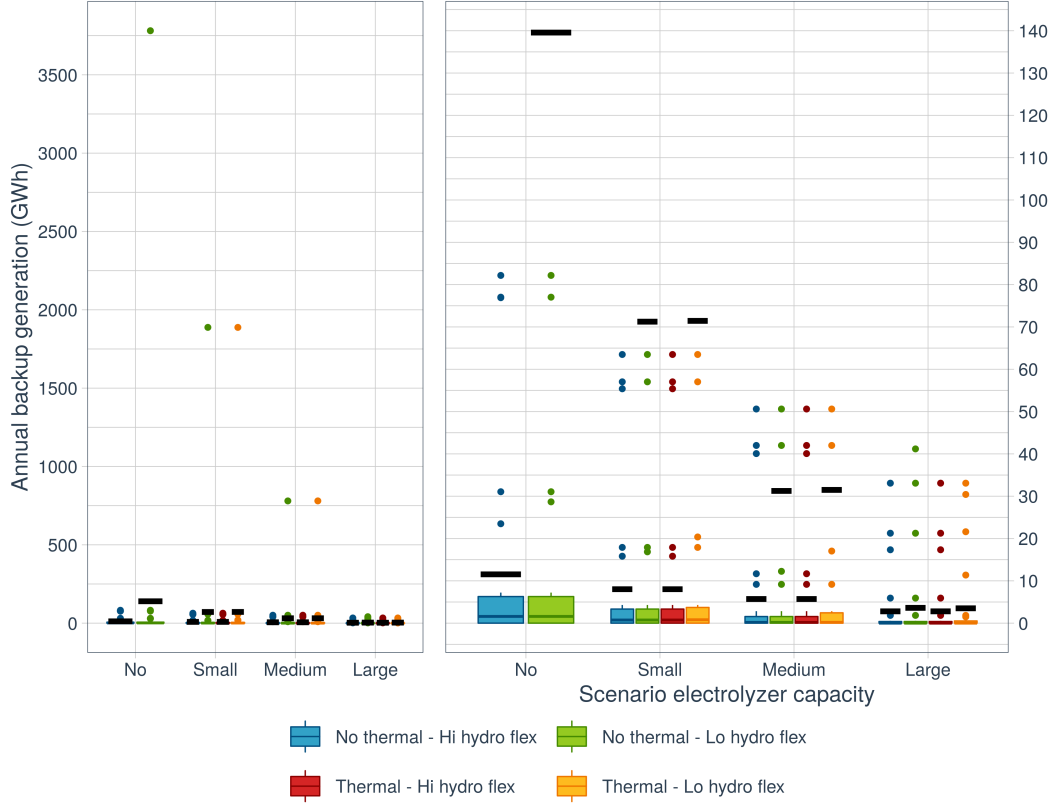


Figure 7: Annual backup energy in all scenarios, the right panel without displaying extreme outliers (1996). Black lines show the mean over all years.

has a perhaps counter-intuitive consequence for the **NO THERMAL** scenarios: at the lower end of electrolyzer capacities, increasing capacities increase the electrolyzer utilization for the **NO THERMAL** scenarios, up to somewhere in the range of 5-10 GW of capacity, depending on the scenario. Above that point, adding more electrolyzer (and wind) capacity, reduces the utilization. The cause is that at lower wind capacities, wind is used to cover residual demand in hours when there is a lot of wind as it is assumed to have zero marginal cost. Less wind is thus available for surplus hydrogen production due to that substitution. Increasing the wind power capacity in the system further will reduce the thermal generation to the defined minimum load, thus making no more substitution of thermal generation possible and instead releasing a higher share of wind power generation for hydrogen production.

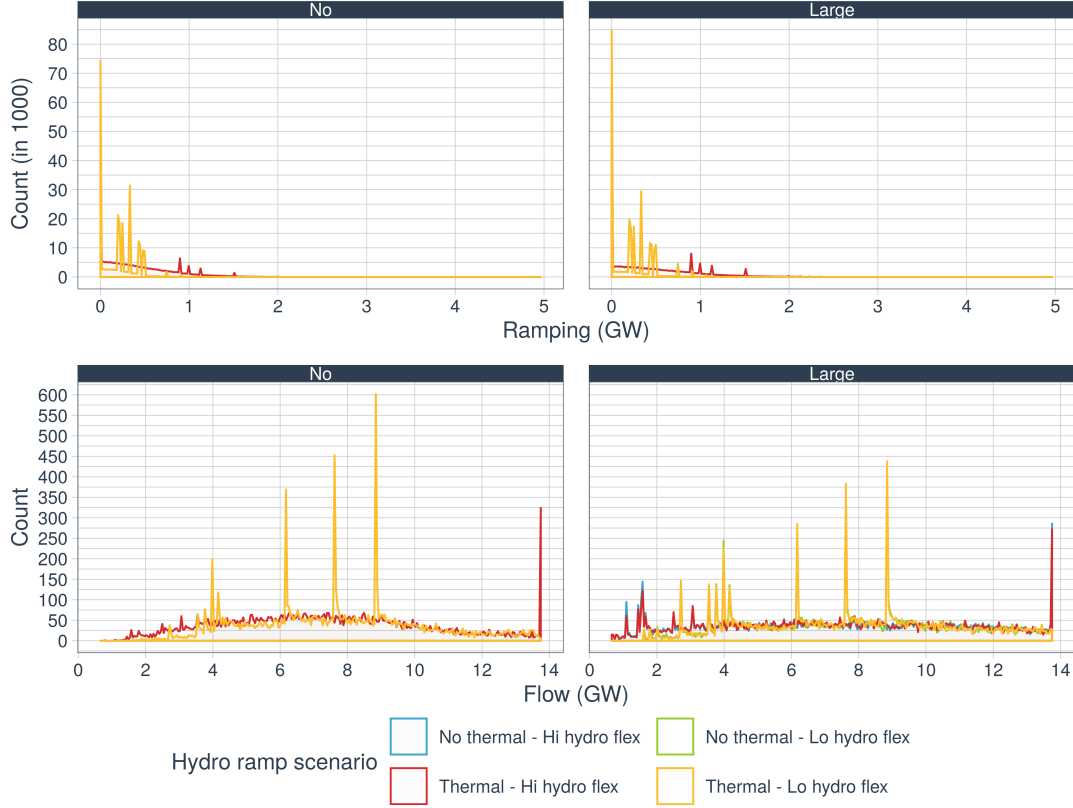


Figure 8: Density plots of hourly flows and ramps over for the hydrogen scenarios **NO** and **LARGE** over all hours.

Therefore, rapidly increasing utilization of electrolyzers can be observed at the lower capacity range in the **NO THERMAL** scenarios. At some point, negative residual demand will exceed the electrolyzer capacity for some hours. Once the latter effect grows stronger than the former, the utilization starts decreasing again. This effect, however, applies only if no extra thermal power is dispatched for hydrogen production. In the **THERMAL** scenario, where thermal power is dispatched for hydrogen production, the utilization starts falling with increasing electrolyzer capacity immediately.

4. Discussion

We have assessed multi-annual variability of hydrogen production in almost fully renewable energy systems, considering flexibility from thermal and hydropower generation. While this has, to the best of our knowledge, not been done before, we discuss here some limitations of our analysis.

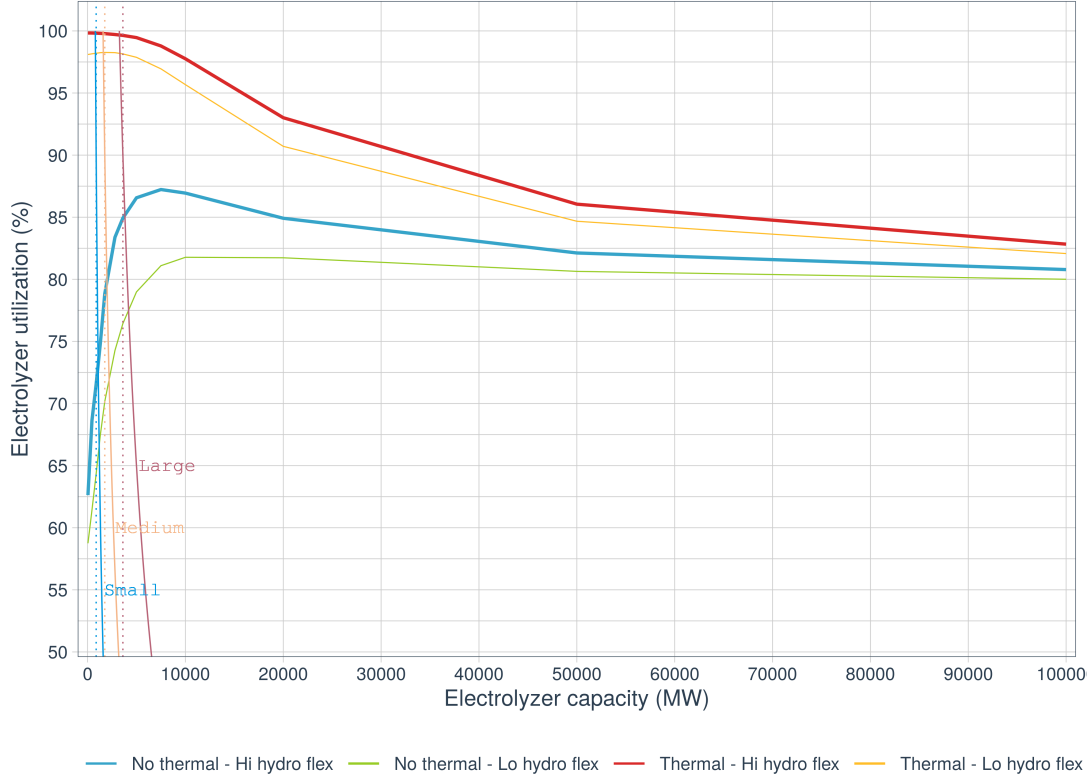


Figure 9: Average electrolyzer full-load operation (%) for an extended electrolyzer capacity range, for all scenarios. The three hydrogen demand scenarios are marked with vertical dotted lines, the curved lines shows the adjusted electrolyzer capacity to meet the expected yearly production (estimated at 90% for each scenario).

The interaction between electricity and hydrogen markets was not modeled. In bad weather years, electricity prices will increase, which will also drive up the hydrogen prices. Depending on the relative effect on the two, markets will either favor thermal dispatch for hydrogen production, thus limiting the negative impact of single bad weather years on hydrogen production, or hydrogen production will decrease.

We also assumed that Sweden has no international interconnections and that internally, there are no transmission bottlenecks. The first assumption makes our results conservative, as the existing interconnections clearly could provide backup capacities. At the same time, market prices and dispatch would change significantly, if interconnections would be taken into consideration. Depending on the thermal flexibility scenario, thermal power generation in neighbouring countries would

be replaced by Swedish wind power generation up to the interconnector capacity, before generating surplus electricity for hydrogen production within the country. Disregard of international interconnections also implies that Sweden has net zero exports and imports, which can be compared to current annual exports of around 10-20 TWh of electricity. The second assumption, which neglects internal restrictions in transmission, is an obvious simplification. Here, we assume that the transmission grid is reinforced to accommodate additional wind power and prevent frequent large-scale curtailment.

Land and sea availability for placing wind-turbines is another major issue. In the scenario with the largest electrolyzer capacity (3610 MW), around 100 TWh of wind power is generated, requiring an installation of around 30 GW of wind power capacity. This compares to an installed capacity of above 50 GW of wind in Germany, a country with only 80% of the available land area of Sweden. Such an expansion should thus in principle be possible. It may, however, cause regional environmental impacts and land conflicts, and mitigation measures must be taken seriously.

We here only considered increased load from electrolysis - other scenarios show a potential increase from electrification of, e.g., transport and (other parts of) industry where total power demand may increase to over 200 TWh a^{-1} , including demand from electrolysis [63]. This compares to a load of about 130 TWh a^{-1} in our scenario without electrolyzer and to around 160 TWh a^{-1} in our largest electrolysis scenario. At the same moment, we assume that around 60 TWh a^{-1} of nuclear are phased out. Keeping nuclear in the system would therefore be able to at least partly cover additional demands from other sectors.

Further, we modelled hydropower operation on an aggregated level for the whole of Sweden. Therefore, detailed assessments of environmental impacts are not possible. Also, some of the dispatch schedules may be physically impossible once down-scaled to the level of river basins. We recommend further work here.

5. Conclusions

We have assessed how electrolyzer operation evolves if a continuous stream of hydrogen should be produced and if power demand of electrolyzers is met on average by new wind power capacities for our Swedish case study. We have shown that while in all scenarios, the average annual utilization

of electrolyzers is above 60%, the inter-annual variability of hydrogen production is high unless thermal power is dispatched for electrolysis.

Furthermore, if hydropower flexibility is additionally restricted to reduce hydropeaking, inter-annual variability is increased further. As the maximum constraints in hydropower generation are, however, only met rarely, one important policy conclusion is that allowing for high, yet rare, extreme operation of hydropower, can make the whole system more resilient. This calls for more research on the ecological impacts of rare hydropeaking events and for a detailed, river-scale assessment of hydropower generation under large penetration of variable renewables.

Due to high inter-annual variability, either long-term storage of hydrogen, backup hydrogen sources or a dispatch of thermal capacities in extreme years is therefore necessary to maintain a stable hydrogen flow to the industry. This means that on average hydrogen costs can be low, but extreme years with high costs have to be expected.

Adding more wind power to the system while also adding large electrolyzer capacity as main consumer of the wind power makes the system more stable, if electrolyzers ramp down in rare hours of extreme events with low availability of renewable generation. The need for additional backup capacities in a fully renewable Swedish power system are reduced in such a system.

We did not explicitly assess the costs of hydrogen production, however, our results, openly available, can provide fundamental input to such kind of analysis by others.

Acknowledgements

The Swedish Research Council Formas (dnr. 2016-20118) and Bio4Energy financially supported this work. We also gratefully acknowledge support from the European Research Council (“reFUEL” ERC2017-STG 758149) and by CLIM2POWER. Project CLIM2POWER is part of ERA4CS, an ERA-NET initiated by JPI Climate, and funded by FORMAS (SE), BMBF (DE), BMWF (AT), FCT (PT), EPA (IE), ANR (FR) with co-funding by the European Union (Grant 690462). We would also like to thank SMHI, the Swedish Meteorological and Hydrological Institute, for providing the S-Hype data.

References

- [1] J. Michalski, M. Poltrum, U. Bünger, The role of renewable fuel supply in the transport sector in a future decarbonized energy system, *International Journal of Hydrogen Energy* 44 (25)

- (2019) 12554–12565. doi:10.1016/j.ijhydene.2018.10.110.
URL <https://linkinghub.elsevier.com/retrieve/pii/S0360319918333093>
- [2] A. Otto, M. Robinius, T. Grube, S. Schiebahn, A. Praktiknjo, D. Stolten, Power-to-steel: Reducing CO₂ through the integration of renewable energy and hydrogen into the German steel industry, *Energies* 10 (4). doi:10.3390/en10040451.
- [3] E. S. Hanley, J. P. Deane, B. P. Gallachóir, The role of hydrogen in low carbon energy futures—A review of existing perspectives, *Renewable and Sustainable Energy Reviews* 82 (3) (2018) 3027–3045. doi:10.1016/j.rser.2017.10.034.
- [4] I. Staffell, D. Scamman, A. Velazquez Abad, P. Balcombe, P. E. Dodds, P. Ekins, N. Shah, K. R. Ward, The role of hydrogen and fuel cells in the global energy system, *Energy and Environmental Science* 12 (2) (2019) 463–491. doi:10.1039/c8ee01157e.
- [5] D. Ferrero, M. Gamba, A. Lanzini, M. Santarelli, Power-to-Gas Hydrogen: Techno-economic Assessment of Processes towards a Multi-purpose Energy Carrier, *Energy Procedia* 101 (September) (2016) 50–57. doi:10.1016/j.egypro.2016.11.007.
URL <http://dx.doi.org/10.1016/j.egypro.2016.11.007><https://linkinghub.elsevier.com/retrieve/pii/S1876610216312164>
- [6] C. J. Quarton, S. Samsatli, The value of hydrogen and carbon capture, storage and utilisation in decarbonising energy: Insights from integrated value chain optimisation, *Applied Energy* 257 (August 2019) (2020) 113936. doi:10.1016/j.apenergy.2019.113936.
URL <https://doi.org/10.1016/j.apenergy.2019.113936><https://linkinghub.elsevier.com/retrieve/pii/S030626191931623X>
- [7] R. McKenna, Q. Bchini, J. Weinand, J. Michaelis, S. König, W. Köppel, W. Fichtner, The future role of Power-to-Gas in the energy transition: Regional and local techno-economic analyses in Baden-Württemberg, *Applied Energy* 212 (2018) 386–400. doi:10.1016/j.apenergy.2017.12.017.
URL <https://linkinghub.elsevier.com/retrieve/pii/S0306261917317312>
- [8] J. Olauson, M. N. Ayob, M. Bergkvist, N. Carpman, V. Castellucci, A. Goude, D. Lingfors, R. Waters, J. Widén, Net load variability in Nordic countries with a highly or fully renewable

- power system, *Nature Energy* 1 (12) (2016) 16175. doi:10.1038/nenergy.2016.175.
URL <http://www.nature.com/articles/nenergy2016175>
- [9] T. W. Brown, T. Bischof-Niemz, K. Blok, C. Breyer, H. Lund, B. V. Mathiesen, Response to ‘Burden of proof: A comprehensive review of the feasibility of 100% renewable-electricity systems’, *Renewable and Sustainable Energy Reviews* 92 (2018) 834–847. doi:10.1016/j.rser.2018.04.113.
URL <http://www.sciencedirect.com/science/article/pii/S1364032118303307>
- [10] L. Hirth, F. Ueckerdt, O. Edenhofer, Integration costs revisited - An economic framework for wind and solar variability, *Renewable Energy* 74 (2015) 925–939. doi:10.1016/j.renene.2014.08.065.
- [11] L. Hirth, The benefits of flexibility: The value of wind energy with hydropower, *Applied Energy* 181 (2016) 210–223. doi:10.1016/j.apenergy.2016.07.039.
- [12] B. Arheimer, G. Lindström, Electricity vs Ecosystems-understanding and predicting hydropower impact on Swedish river flow, *IAHS-AISH Proceedings and Reports* 364 (2014) 313–319. doi:10.5194/piahs-364-313-2014.
- [13] F. B. Ashraf, A. T. Haghighi, J. Riml, K. Alfredsen, J. J. Koskela, B. Kløve, H. Marttila, Changes in short term river flow regulation and hydropeaking in Nordic rivers, *Scientific Reports* 8 (1) (2018) 1–12. doi:10.1038/s41598-018-35406-3.
- [14] M. D. Bejarano, R. Jansson, C. Nilsson, The effects of hydropeaking on riverine plants: a review, *Biological Reviews* 93 (1) (2018) 658–673. doi:10.1111/brv.12362.
URL <http://doi.wiley.com/10.1111/brv.12362>
- [15] B. M. Renöfält, R. Jansson, C. Nilsson, Effects of hydropower generation and opportunities for environmental flow management in Swedish riverine ecosystems, *Freshwater Biology* 55 (1) (2010) 49–67. doi:10.1111/j.1365-2427.2009.02241.x.
URL <http://doi.wiley.com/10.1111/j.1365-2427.2009.02241.x>
- [16] J. D. Kern, D. Patino-Echeverri, G. W. Characklis, The Impacts of Wind Power Integration on Sub-Daily Variation in River Flows Downstream of Hydroelectric Dams, *Environmental Science & Technology* 48 (16) (2014) 9844–9851, publisher: American Chemical Society. doi:

10.1021/es405437h.

URL <https://doi.org/10.1021/es405437h>

- [17] C. Graf, C. Marcantonini, Renewable energy and its impact on thermal generation, *Energy Economics* 66 (2017) 421–430. doi:10.1016/j.eneco.2017.07.009.
URL <http://www.sciencedirect.com/science/article/pii/S0140988317302463>
- [18] C. Oberschelp, S. Pfister, C. E. Raptis, S. Hellweg, Global emission hotspots of coal power generation, *Nature Sustainability* 2 (2) (2019) 113–121, number: 2 Publisher: Nature Publishing Group. doi:10.1038/s41893-019-0221-6.
URL <https://www.nature.com/articles/s41893-019-0221-6>
- [19] B. Holtsmark, The outcome is in the assumptions: analyzing the effects on atmospheric CO₂ levels of increased use of bioenergy from forest biomass, *GCB Bioenergy* 5 (4) (2013) 467–473, eprint: <https://onlinelibrary.wiley.com/doi/pdf/10.1111/gcbb.12015>. doi:10.1111/gcbb.12015.
URL <https://onlinelibrary.wiley.com/doi/abs/10.1111/gcbb.12015>
- [20] J. Schmidt, K. Gruber, M. Klingler, C. Klöckl, L. R. Camargo, P. Regner, O. Turkovska, S. Wehrle, E. Wetterlund, A new perspective on global renewable energy systems: why trade in energy carriers matters, *Energy & Environmental Science* 12 (7) (2019) 2022–2029. doi:10.1039/C9EE00223E.
URL <https://pubs.rsc.org/en/content/articlelanding/2019/ee/c9ee00223e>
- [21] P. Caumon, M. Lopez-Botet Zulueta, J. Louyrette, S. Albou, C. Bourasseau, C. Mansilla, Flexible hydrogen production implementation in the French power system: Expected impacts at the French and European levels, *Energy* 81 (2015) 556–562. doi:10.1016/j.energy.2014.12.073.
URL <http://www.sciencedirect.com/science/article/pii/S0360544215000055>
- [22] E. F. Bødal, M. Korpås, Value of hydro power flexibility for hydrogen production in constrained transmission grids, *International Journal of Hydrogen Energy* 45 (2) (2020) 1255–1266. doi:10.1016/j.ijhydene.2019.05.037.
URL <http://www.sciencedirect.com/science/article/pii/S0360319919318671>

- [23] D. Wang, M. Muratori, J. Eichman, M. Wei, S. Saxena, C. Zhang, Quantifying the flexibility of hydrogen production systems to support large-scale renewable energy integration, *Journal of Power Sources* 399 (2018) 383–391. doi:10.1016/j.jpowsour.2018.07.101.
URL <http://www.sciencedirect.com/science/article/pii/S0378775318308267>
- [24] Y. Li, W. Gao, Y. Ruan, Potential and sensitivity analysis of long-term hydrogen production in resolving surplus RES generation—a case study in Japan, *Energy* 171 (2019) 1164–1172. doi:10.1016/j.energy.2019.01.106.
URL <http://www.sciencedirect.com/science/article/pii/S0360544219301070>
- [25] J. Haas, W. Nowak, R. Palma-Behnke, Multi-objective planning of energy storage technologies for a fully renewable system: Implications for the main stakeholders in Chile, *Energy Policy* 126 (2019) 494–506. doi:10.1016/j.enpol.2018.11.034.
URL <http://www.sciencedirect.com/science/article/pii/S0301421518307651>
- [26] D. Lu, B. Wang, Y. Wang, H. Zhou, Q. Liang, Y. Peng, T. Roskilly, Optimal operation of cascade hydropower stations using hydrogen as storage medium, *Applied Energy* 137 (2015) 56–63. doi:10.1016/j.apenergy.2014.09.092.
URL <http://www.sciencedirect.com/science/article/pii/S030626191401040X>
- [27] M. Robinius, A. Otto, K. Syranidis, D. S. Ryberg, P. Heuser, L. Welder, T. Grube, P. Markewitz, V. Tietze, D. Stolten, Linking the Power and Transport Sectors—Part 2: Modelling a Sector Coupling Scenario for Germany, *Energies* 10 (7) (2017) 957, number: 7 Publisher: Multidisciplinary Digital Publishing Institute. doi:10.3390/en10070957.
URL <https://www.mdpi.com/1996-1073/10/7/957>
- [28] L. Bolívar Jaramillo, A. Weidlich, Optimal microgrid scheduling with peak load reduction involving an electrolyzer and flexible loads, *Applied Energy* 169 (2016) 857–865. doi:10.1016/j.apenergy.2016.02.096.
URL <http://www.sciencedirect.com/science/article/pii/S0306261916302525>
- [29] M. Robinius, T. Raje, S. Nykamp, T. Rott, M. Müller, T. Grube, B. Katzenbach, S. Küppers, D. Stolten, Power-to-Gas: Electrolyzers as an alternative to network expansion – An example from a distribution system operator, *Applied Energy* 210 (2018) 182–197. doi:10.1016/j.

- apenergy.2017.10.117.
URL <http://www.sciencedirect.com/science/article/pii/S0306261917315623>
- [30] M. Fasihi, D. Bogdanov, C. Breyer, Long-Term Hydrocarbon Trade Options for the Maghreb Region and Europe—Renewable Energy Based Synthetic Fuels for a Net Zero Emissions World, *Sustainability* 9 (2) (2017) 306. doi:10.3390/su9020306.
URL <http://www.mdpi.com/2071-1050/9/2/306>
- [31] M. Fasihi, D. Bogdanov, C. Breyer, Techno-Economic Assessment of Power-to-Liquids (PtL) Fuels Production and Global Trading Based on Hybrid PV-Wind Power Plants, *Energy Procedia* 99 (2016) 243–268. doi:10.1016/j.egypro.2016.10.115.
URL <http://www.sciencedirect.com/science/article/pii/S1876610216310761>
- [32] A. Gulagi, D. Bogdanov, M. Fasihi, C. Breyer, Can Australia Power the Energy-Hungry Asia with Renewable Energy?, *Sustainability* 9 (2) (2017) 233. doi:10.3390/su9020233.
URL <https://www.mdpi.com/2071-1050/9/2/233>
- [33] Swedish Government, Framework agreement between the Swedish Social Democratic Party, the Moderate Party, the Swedish Green Party, the Centre Party and the Christian Democrats (2016).
URL <https://www.government.se/articles/2016/06/agreement-on-swedish-energy-policy/>
- [34] Swedish Energy Agency, Swedish Agency for Marine and Water Management, Strategy for measures in the hydropower (Strategi för åtgärder i vattenkraften - Avvägning mellan energimål och miljö kvalitetsmålet Levande sjöar och vattendrag , in Swedish), Tech. rep., The Swedish Agency for Marine and Water Management, Göteborg, Sweden (2014).
URL www.havochvatten.se
- [35] M. D. Bejarano, Á. Sordo-Ward, C. Alonso, C. Nilsson, Characterizing effects of hydropower plants on sub-daily flow regimes, *Journal of Hydrology* 550 (2017) 186–200. doi:10.1016/j.jhydrol.2017.04.023.
URL <https://linkinghub.elsevier.com/retrieve/pii/S0022169417302433>
- [36] IVA, Future Electricity Production in Sweden, IVA Electricity Crossroads project, Tech. rep., The Royal Swedish Academy of Engineering Sciences (IVA), Stockholm, Sweden (2017).

URL <https://www.iva.se/globalassets/rapporter/vagval-el/201705-iva-vagvalel-framtidens-elproduktion-english-c.pdf>

- [37] Swedish Energy Agency, 100 percent renewable electricity. Part report 2 (100 procent förnybar el. Delrapport 2 - Scenarier, vägval och utmaningar, in Swedish), Tech. rep., Swedish Energy Agency, Eskilstuna, Sweden (2019).
- [38] Jernkontoret, Climate roadmap for a fossil-free and competitive steel industry in Sweden, Tech. rep., Jernkontoret, Stockholm, Sweden (2018).
- [39] B. Petrol, BP Statistical Review of World Energy 2019, Tech. rep. (2019).
- [40] J. Schmidt, R. Cancella, A. O. Pereira Jr., An optimal mix of solar PV, wind and hydro power for a low-carbon electricity supply in Brazil, *Renewable Energy* 85 (2016) 137–147. doi:10.1016/j.renene.2015.06.010.
URL <http://www.sciencedirect.com/science/article/pii/S0960148115300331>
- [41] S. Höltinger, C. Mikovits, J. Schmidt, J. Baumgartner, B. Arheimer, G. Lindström, E. Wetterlund, The impact of climatic extreme events on the feasibility of fully renewable power systems: A case study for Sweden, *Energy* 178 (2019) 695–713. doi:10.1016/j.energy.2019.04.128.
URL <https://linkinghub.elsevier.com/retrieve/pii/S0360544219307613>
- [42] C. Jung, D. Taubert, D. Schindler, The temporal variability of global wind energy – Long-term trends and inter-annual variability, *Energy Conversion and Management* 188 (2019) 462–472. doi:10.1016/j.enconman.2019.03.072.
URL <http://www.sciencedirect.com/science/article/pii/S0196890419303760>
- [43] M. Zeyringer, J. Price, B. Fais, P.-H. Li, E. Sharp, Designing low-carbon power systems for Great Britain in 2050 that are robust to the spatiotemporal and inter-annual variability of weather, *Nature Energy* 3 (5) (2018) 395–403. doi:10.1038/s41560-018-0128-x.
URL <http://dx.doi.org/10.1038/s41560-018-0128-x>
<http://www.nature.com/articles/s41560-018-0128-x>
- [44] C. Mikovits, S. Höltinger, J. Schmidt, RE_EXTREME Simulation, Data, and Results (2020). doi:10.5281/zenodo.3712940.
URL <https://zenodo.org/record/3712940>

- [45] J. Olauson, M. Bergkvist, Modelling the Swedish wind power production using MERRA reanalysis data, *Renewable Energy* 76 (2015) 717–725. doi:10.1016/j.renene.2014.11.085.
URL <http://dx.doi.org/10.1016/j.renene.2014.11.085><https://linkinghub.elsevier.com/retrieve/pii/S0960148114008167>
- [46] J. Olauson, H. Bergström, M. Bergkvist, Scenarios and time series of future wind power production in Sweden, Tech. rep., Uppsala University, Uppsala (2015).
- [47] Swedenergy, The energy year 2018 - Electricity production (Energiåret 2018 - Elproduktion, in Swedish) (2019).
- [48] G. Lindström, C. Pers, J. Rosberg, J. Strömqvist, B. Arheimer, Development and testing of the HYPE (Hydrological Predictions for the Environment) water quality model for different spatial scales, *Hydrology Research* 41 (3-4) (2010) 295–319. doi:10.2166/nh.2010.007.
URL <http://hr.iwaponline.com/cgi/doi/10.2166/nh.2010.007><https://iwaponline.com/hr/article/41/3-4/295/822/Development-and-testing-of-the-HYPE-Hydrological>
- [49] J. Strömqvist, B. Arheimer, J. Dahné, C. Donnelly, G. Lindström, Water and nutrient predictions in ungauged basins: set-up and evaluation of a model at the national scale, *Hydrological Sciences Journal* 57 (2) (2012) 229–247. doi:10.1080/02626667.2011.637497.
URL <http://www.tandfonline.com/doi/abs/10.1080/02626667.2011.637497><https://www.tandfonline.com/doi/full/10.1080/02626667.2011.637497>
- [50] Swedenergy, The energy year 2017 - Electricity production (Energiåret 2017 - Elproduktion, in Swedish), Tech. rep., Stockholm, Sweden (2018).
- [51] Platts, UDI World Electric Power Plants Database (WEPP), Tech. rep. (2016).
- [52] Bioenergi, Bio-power in Sweden (Biokraft i Sverige) 2018, Tech. rep. (2018).
URL <https://bioenergitidningen.se/e-tidning-kartor/biokraft-i-sverige>
- [53] Swedenergy, Statistics over fuels and deliveries in Swedish district heating systems 2015-2017, Tech. rep., Stockholm, Sweden (2018).
URL <https://www.energiforetagen.se/statistik/fjarrvarmestatik/tillford-energi/>

- [54] I. Nohlgren, S. Herstad Svärd, M. Jansson, J. Rodin, El från nya och framtida anläggningar 2014, Tech. rep., Elforsk, Stockholm (2014).
- [55] The investment costs of electrolysis – A comparison of cost studies from the past 30 years, International Journal of Hydrogen Energy 43 (3) (2018) 1209–1223. doi:10.1016/j.ijhydene.2017.11.115.
- [56] O. Schmidt, A. Gambhir, I. Staffell, A. Hawkes, J. Nelson, S. Few, Future cost and performance of water electrolysis: An expert elicitation study, International Journal of Hydrogen Energy 42 (52) (2017) 30470–30492. doi:10.1016/j.ijhydene.2017.10.045.
URL <https://doi.org/10.1016/j.ijhydene.2017.10.045>
- [57] L. Bertuccioli, A. Chan, D. Hart, F. Lehner, B. Madden, E. Standen, Development of Water Electrolysis in the European Union - Final report, Tech. rep., E4tech Sàrl and element energy, Lausanne, Switzerland and Cambridge, UK (2014).
URL www.e4tech.com
- [58] Preem, Preem annual report 2018, Tech. rep. (2019).
URL https://www.preem.se/globalassets/om-preem/finansuell-info/arsredovisningar/2018/preem{}_annual-report-2018{}_eng.pdf
- [59] J. A. Melero, J. Iglesias, A. Garcia, Biomass as renewable feedstock in standard refinery units. Feasibility, opportunities and challenges, Energy & Environmental Science 5 (6) (2012) 7393. doi:10.1039/c2ee21231e.
URL <http://xlink.rsc.org/?DOI=c2ee21231e>
- [60] S. Karatzos, J. D. Mcmillan, J. N. Saddler, The Potential and Challenges of Drop-in Biofuels, Tech. rep. (2014).
URL <http://task39.sites.olt.ubc.ca/files/2014/01/Task-39-Drop-in-Biofuels-Report-FINAL-2-Oct-2014.pdf>
- [61] D. Kushnir, T. Hansen, V. Vogl, M. Åhman, Adopting hydrogen direct reduction for the Swedish steel industry: A technological innovation system (TIS) study, Journal of Cleaner Production 242. doi:10.1016/j.jclepro.2019.118185.

- [62] M. A. Olivares, J. Haas, R. Palma-Behnke, C. Benavides, A framework to identify Pareto-efficient subdaily environmental flow constraints on hydropower reservoirs using a grid-wide power dispatch model, *Water Resources Research* 51 (5) (2015) 3664–3680. doi:10.1002/2014WR016215.
URL <https://onlinelibrary.wiley.com/doi/abs/10.1002/2015WR017200http://doi.wiley.com/10.1002/2014WR016215>
- [63] IVA, How the Swedish energy system manages the climate targets (Så klarar det svenska energisystemet klimatmålen, in Swedish), Tech. Rep. September, The Royal Swedish Academy of Engineering Sciences (IVA), Stockholm, Sweden (2019).
URL <https://www.iva.se/globalassets/bilder/projekt/vagval-klimat/201910-iva-vagval-for-klimatet-delrapport5-g.pdf>
- [64] IEA/NEA, Projected Costs of Generating Electricity, 2015 Edition, Tech. rep., International Energy Agency (IEA) and Nuclear Energy Agency (NEA), Paris, France (2015).
URL <https://webstore.iea.org/projected-costs-of-generating-electricity-2015>
- [65] Sveriges Riksbank, Exchange rates, annual average 2018 (2019).
URL <https://www.riksbank.se/en-gb/statistics/search-interest--exchange-rates/annual-average-exchange-rates/>
- [66] J. Gode, F. Martinsson, L. Hagberg, A. Öman, J. Höglund, D. Palm, Miljöfaktaboken 2011 - Estimated emission factors for fuels, electricity, heat and transport in Sweden (in Swedish), Tech. Rep. Report 1183, Stockholm (2011).
- [67] Eurostat, Gas prices for non-household consumers (2018).
URL https://appsso.eurostat.ec.europa.eu/nui/show.do?dataset=nrg_{_}pc_{_}203{&}lang=en
- [68] Swedish Energy Agency, Wood fuel- and peat prices, quarterly, 1993- (2019).
- [69] European Commission, EU Weekly Oil Bulletin (2018).
URL <https://ec.europa.eu/energy/en/data-analysis/weekly-oil-bulletin>

Appendix A. Model description

We employ a deterministic model to optimize the dispatch of hydropower and thermal power production. The model determines system costs minimizing the hourly dispatch costs of thermal power plants, while meeting the hourly demand.

Appendix A.1. Mathematical description

Appendix A.1.1. Objective

The objective function is given by equation A.1, which represents dispatch costs *dispatch_costs* in the system over one year.

$$\begin{aligned} \min_{dispatch_costs} \sum_h & \left(x_hydro_h \cdot c_{hy} + x_spill_h \cdot c_s + \sum_{type} (x_thermal_{h,type} \cdot c_{th,type}) \right. \\ & \left. + x_backup_dispatch_h \cdot c_{bd} - x_h2_h \cdot p_{h2} \right) \end{aligned} \quad (A.1)$$

The costs are given by the sum of dispatching thermal power production ($x_thermal_{h,type}$) with cost $c_{th,type}$, and dispatching backup generation $x_backup_dispatch_h$ with cost c_{bd} . We also assign costs to hydropower production x_hydro_h and to spilling of water x_spill_h . These costs are set very low and represent the future value of water. As the produced hydrogen x_h2_h has a market value p_{h2} , it enters negatively into the objective function.

Appendix A.1.2. Constraints

The residual demand $demand_h$, potential curtailments $x_curtailment_h$, and hydrogen production has to be met in all time instances by generation of hydropower and thermal power as shown in equation A.2.

$$\begin{aligned} demand_h = x_hydro_h + \sum_{type} (x_thermal_{h,type}) + x_backup_demand_h \\ - x_curtailment_h - x_h2_h \quad \forall h \end{aligned} \quad (A.2)$$

Installed capacities of thermal power plants $thcap_{type}$ and electrolyers $h2cap$ are defined in equations eqs. (A.3) and (A.4).

$$x_{thermal_{h,type}} \leq thcap_{type} \quad \forall h \quad (\text{A.3})$$

$$x_{h2_h} \leq h2cap \quad \forall h \quad (\text{A.4})$$

Additional constraints for hydro flow, ramping and the storage level are controlled with the following equations:

Equation A.5 ensures that the reservoir level $x_{reservoir_level_h}$ of one specific hour equals the reservoir level of the previous hour, plus the natural inflow $natural_inflow_h$, minus the outflow (hydropower production x_{hydro_h} and spill x_{spill_h}).

$$\begin{aligned} x_{reservoir_level_h} = & x_{reservoir_level_{h-1}} + natural_inflow_h \\ & - x_{hydro_h} - x_{spill_h} \end{aligned} \quad \forall h \quad (\text{A.5})$$

The reservoir level $x_{reservoir_level_h}$ at the end of each simulated year is controlled by equation A.6, which ensures that the level is above $min_endstorage$.

$$x_{reservoir_level_h} \geq min_endstorage \quad h \in \{8760\} \quad (\text{A.6})$$

The minimum flow in each hour is controlled by equation A.7, which ensures that hydropower production x_{hydro_h} and hydro spilling x_{spill_h} is larger than the minimum flow min_flow_h .

$$x_{hydro_h} + x_{spill_h} \geq min_flow_h \quad \forall h \quad (\text{A.7})$$

Likewise, the maximum possible flow max_flow_h is defined by equation A.8.

$$x_{hydro_h} + x_{spill_h} \leq max_flow_h \quad \forall h \quad (\text{A.8})$$

The maximum change in total flow per hour (maximum ramping, MRR) $max_hydro_ramp_h$ is defined by equations A.9 and A.10.

$$x_{hydro_h} + x_{spill_h} - x_{hydro_{h-1}} - x_{spill_{h-1}} \leq max_hydro_ramp_h \quad \forall h \quad (\text{A.9})$$

$$x_{hydro_{h-1}} + x_{spill_{h-1}} - x_{hydro_h} - x_{spill_h} \leq max_hydro_ramp_h \quad \forall h \quad (\text{A.10})$$

Maximum ramping $max_hydro_prod_ramp$ of hydropower production x_hydro_h is controlled by equations A.11 and A.12.

$$x_hydro_h - x_hydro_{h-1} \leq max_hydro_prod_ramp \quad \forall h \quad (\text{A.11})$$

$$x_hydro_{h-1} - x_hydro_h \leq max_hydro_prod_ramp_h \quad \forall h \quad (\text{A.12})$$

Restrictions of thermal generation $x_thermal_{h,type}$ are defined by the following equations. Minimum $min_thermal_{h,type}$ and maximum $max_thermal_{h,type}$ thermal generation by type are controlled by equations A.13 and A.14.

$$x_thermal_{h,type} \geq min_thermal_{h,type} \quad \forall h, type \quad (\text{A.13})$$

$$x_thermal_{h,type} \leq max_thermal_{h,type}, \quad \forall h, type \quad (\text{A.14})$$

Thermal ramping, summed over all types, is constrained by equations A.15 and A.16 .

$$\begin{aligned} \sum_{type} (x_thermal_{h,type}) - \sum_{type} (x_thermal_{h-1,type}) \\ \leq max_thermal_ramp_h \quad \forall h \end{aligned} \quad (\text{A.15})$$

$$\begin{aligned} \sum_{type} (x_thermal_{h-1,type}) - \sum_{type} (x_thermal_{h,type}) \\ \leq max_thermal_ramp_h \quad \forall h \end{aligned} \quad (\text{A.16})$$

The hourly wind production $wind_h$ restricts wind curtailment $x_curtailment_h$ in equation A.17, wind can thus be curtailed from 0% to 100%.

$$x_curtailment_h \leq wind_h \quad \forall h \quad (\text{A.17})$$

Appendix A.1.3. Parameters

Table A.3 summarises the used hourly data, parameters and variables.

Table A.3: Hourly data, parameters and variables used.

	Name	Symbol	Unit	Value
Hourly data	Residual demand	$demand_h$	MW	see section 2.1.1
	Natural in flow	$natural_inflow_h$	MW	see section 2.1.3
	Wind production	$wind_h$	MW	see section 2.1.2
Costs & Values	Costs hydro generation	c_{hy}	€MWh ⁻¹	0.1
	Costs hydro spilling	c_s	€MWh ⁻¹	0.05
	Costs thermal generation by type	$c_{th,type}$	€MWh ⁻¹	see table A.4
	Costs backup generation	c_{bd}	€MWh ⁻¹	1500
	Value hydrogen production	p_{h2}	€MWh ⁻¹	18 160
Capacities, Ramps & Restrictions	Thermal capacity by type	$thcap_{type}$	MW	see table 1
	Electrolysis capacity	$elcap$	MW	see table 2
	Minimum endstorage	$min_endstorage$	MW	60 % of Reservoir capacity
	Reservoir capacity	-	MWh	33,700,000
	Minimum hydro flow	min_flow	MW	see figure 2
	Maximum hydro flow	min_flow	MW	see figure 2
	Maximum hydro production ramp	$max_hydro_prod_ramp$	MW	4000
	Minimum thermal production by type	$min_thermal_{h,type}$	MW	see figure 1
	Maximum thermal production by type	$max_thermal_{h,type}$	MW	see figure 1
	Maximum thermal ramping	$max_thermal_ramp_h$	MW	1500

Appendix A.2. Input data for thermal power production costs

Table A.4 summarizes the key plant data used to calculate the thermal power production costs, and table A.5 the fuel costs and fuel-related CO₂ emission factors.

Power production costs were set based on bottom-up technology and fuel specific projections of electricity generation costs [54, 64], and were adjusted to €₂₀₁₈ using the average 2018 currency exchange rate of 1 € = 10.3 SEK [65] and updated fuel prices. The production costs include fuel costs including a CO₂-charge (50 €/ton_{CO₂}), costs for operation and maintenance (O&M), and heat credits, when applicable.

Table A.4: Technical data for the modelled thermal power plants [54, 64]. CHP = combined heat and power, RDF = refuse derived fuel, NG = natural gas, NGCC = natural gas combined cycle, FST = condensing steam turbine, OCGT = open cycle gas turbine, IC = internal combustion engine, S = small, M = medium, L = large, I = industrial. See table 1 for additional details.

Production type	Power prod. (MW)	Heat prod. (MW)	El. efficiency (%)	Alfa value	Var. O&M (€ MWh ⁻¹ fuel)	Fixed O&M (€ MWh ⁻¹ el.)
Waste (CHP)	20	78	20	0.256	5.26	215
RDF (CHP)	20	70	22	0.286	5.46	166
Biomass I (CHP)	80	180	33	0.444	2.63	37.0
Biomass L (CHP) ^a	80	180	33	0.444	2.63	37.0
Biomass M (CHP)	30	72	32	0.417	2.53	56.5
Biomass S (CHP)	10	28	28	0.357	2.44	89.7
NGCC-L (CHP)	150	115	53	1.30	0.78	19.5
NGCC-M (CHP)	40	35	49	1.14	0.97	29.2
NG-IC (CHP)	1	1.2	41	0.833	3.9	0
Oil/NG FST	300	0	38	-	4.66	14.3
Oil OCGT	300	0	34	-	5.21	10.1
Biogas IC (CHP)	1	1.2	41	0.833	3.9	0

^a This category also contains CHP plants currently using coal or peat as fuel (total installed capacity of 298 MW), as those were assumed to have been replaced by biomass CHP.

Table A.5: Energy carrier costs and CO₂ emission factors.

Energy carrier	Price (€MWh ⁻¹)	CO ₂ emissions (kg CO ₂ /MWh) [66]	Price source
NG (≤ 5 MWbr)	39	205.2	[67]
NG (≤ 150 MWbr)	33	205.2	[67]
NG (≥ 150 MWbr)	27	205.2	[67]
Biogas	79	0	[54]
Woody biomass	20	0	[68]
Waste	-12	133.2	[54]
RDF	2.5	86.4	[54]
Oil	36	266.4	[69]
Heat, large plants	-24.4	-	[54]
Heat, small plants	-39	-	[54]

Appendix A.3. Detailed results on thermal power production and need for backup capacity

Figure A.10 shows load duration curves of the resulting dispatched thermal generation in two of the analysed hydrogen demand scenarios (**NO** and **LARGE**), for both **NO THERMAL** and **THERMAL**, and for the two hydropower flexibility scenarios. The curves are derived from all 29 weather years (total of about 254,000 hours).

The left column always shows lower thermal generation than the right column, indicating that decreasing hydropower flexibility will increase thermal dispatch. The first row shows a situation without electrolyzers. Thermal power production is dominated by biomass generation, with a small base-load production from waste incineration. Here, biomass plants and partly peaking plants from natural gas and oil are dispatched to balance wind power in the system.

The mid row shows the **NO THERMAL** scenarios for a **LARGE** electrolyzer capacity. It is a situation where thermal generation is at its almost constrained minimum, as it is not dispatched for hydrogen production and wind power capacities in the system are high. Natural gas and oil plants are almost not dispatched.

In the bottom row the **THERMAL** scenarios for the **LARGE** electrolyzer capacity scenarios are shown. The dispatch of biomass capacities is significantly increased here, as well as peaking natural



Figure A.10: Resulting thermal power load duration curves, per production type (aggregated), on hourly basis over all 29 years. Top: No hydrogen scenario, middle: LARGE in combination with NO THERMAL, bottom: LARGE hydrogen in combination with THERMAL. Left: HI HYDRO FLEX , right: LO HYDRO FLEX.

gas and oil plants. This indicates that to achieve high utilization of electrolyzers in some years fossil generation has to be extensively dispatched (up to 5 TWh) to guarantee hydrogen supply. However, as a share of total thermal generation, fossil generation is very low in all scenarios and never ultrapasses 1 TWh of annual generation on average over all 29 weather years.

Figure A.11 shows the required backup capacity for the same six scenarios as a load duration curve. The figure thus shows the parts of the residual demand not covered by thermal and hydropower generation. The differences in the need for backup capacities between scenarios are similar to the patterns observed for thermal power production. In general, both the capacities and the utilization are low. In the No hydrogen scenario, about 6000 MW of backup capacity is required for a few hours, which is reduced to just above 2000 MW in the LARGE hydrogen scenario. The

capacities are dispatched for very few hours in the whole period - just over 1% of all hours in the baseline scenario, which drops to less than 0.1% in the **LARGE** hydrogen scenario.

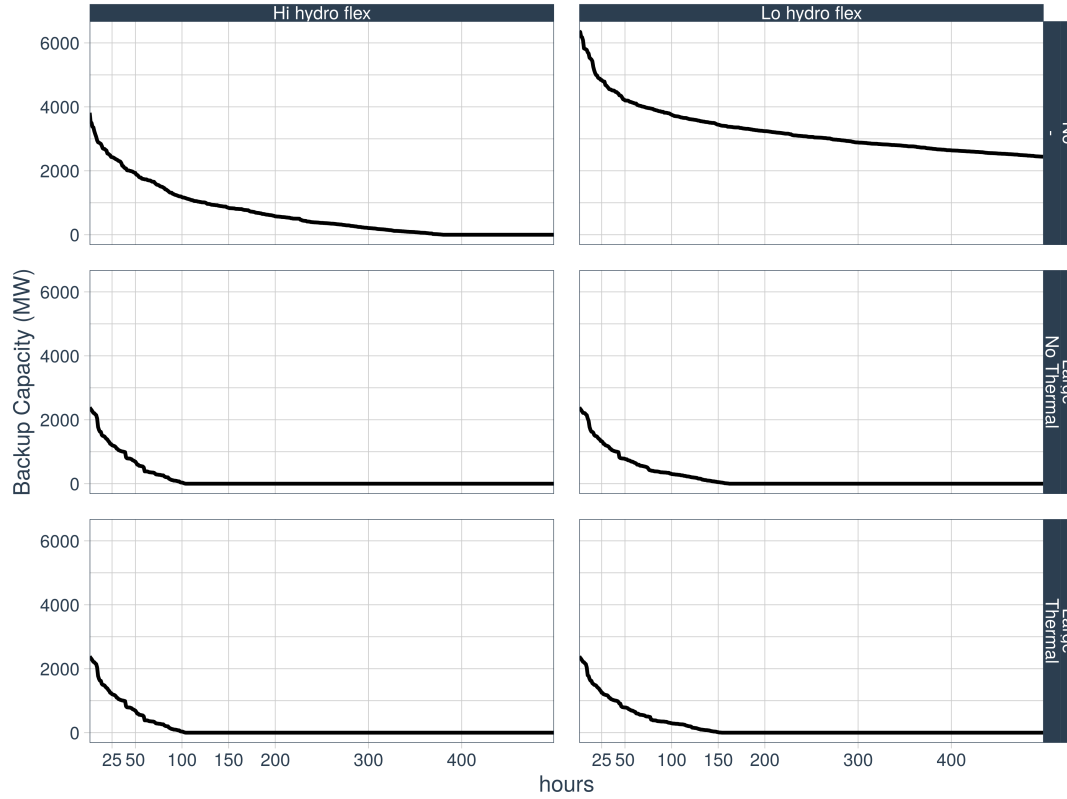


Figure A.11: Load duration curves for additional backup capacity. Top: **NO** hydrogen, middle: **LARGE** hydrogen and **NO THERMAL**, bottom: **LARGE** hydrogen with **THERMAL**. Left: **HI HYDRO FLEX**, right **LO HYDRO FLEX**.

Appendix A.4. Detailed results on hydropower ramping and minimum flows

The distribution of hourly river flows and ramps are already shown in section 3.4. Here we show the results for all scenarios on the distribution of hydropower ramps (A.12) and hydropower flows n (A.13) in detail.

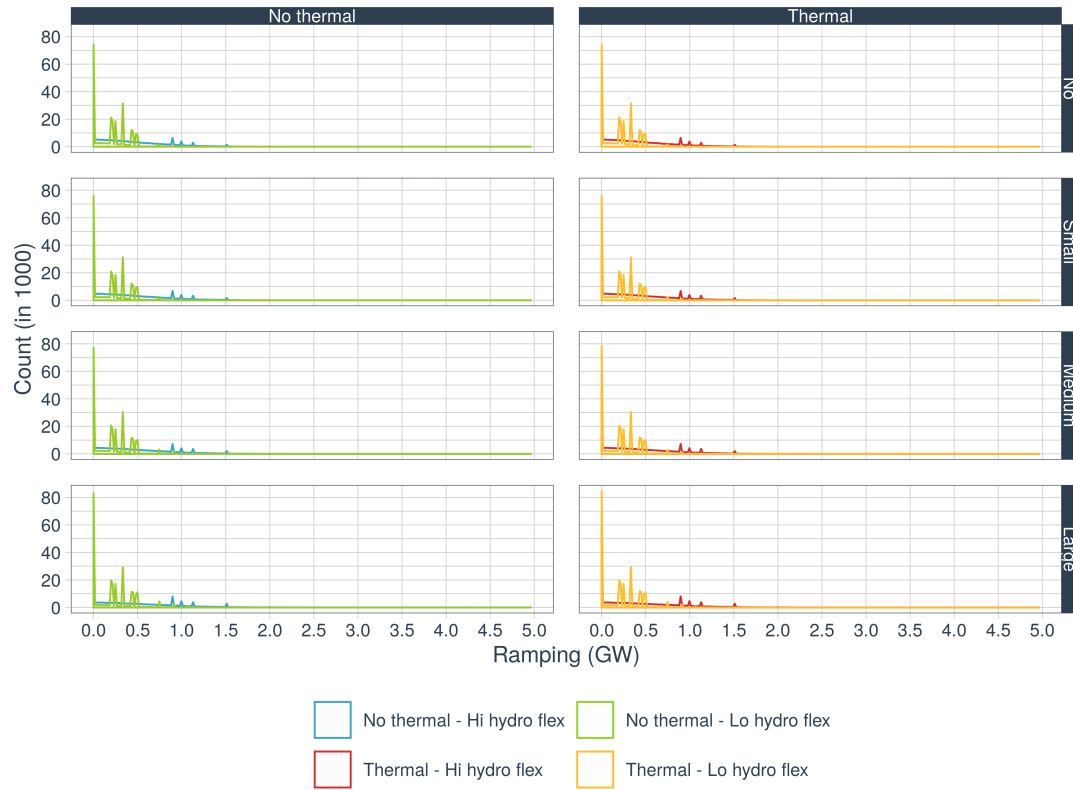


Figure A.12: Density plots of hourly hydro ramps over for all scenarios. Panels left NO THERMAL and right THERMAL, from top to bottom: electrolyzer capacity.

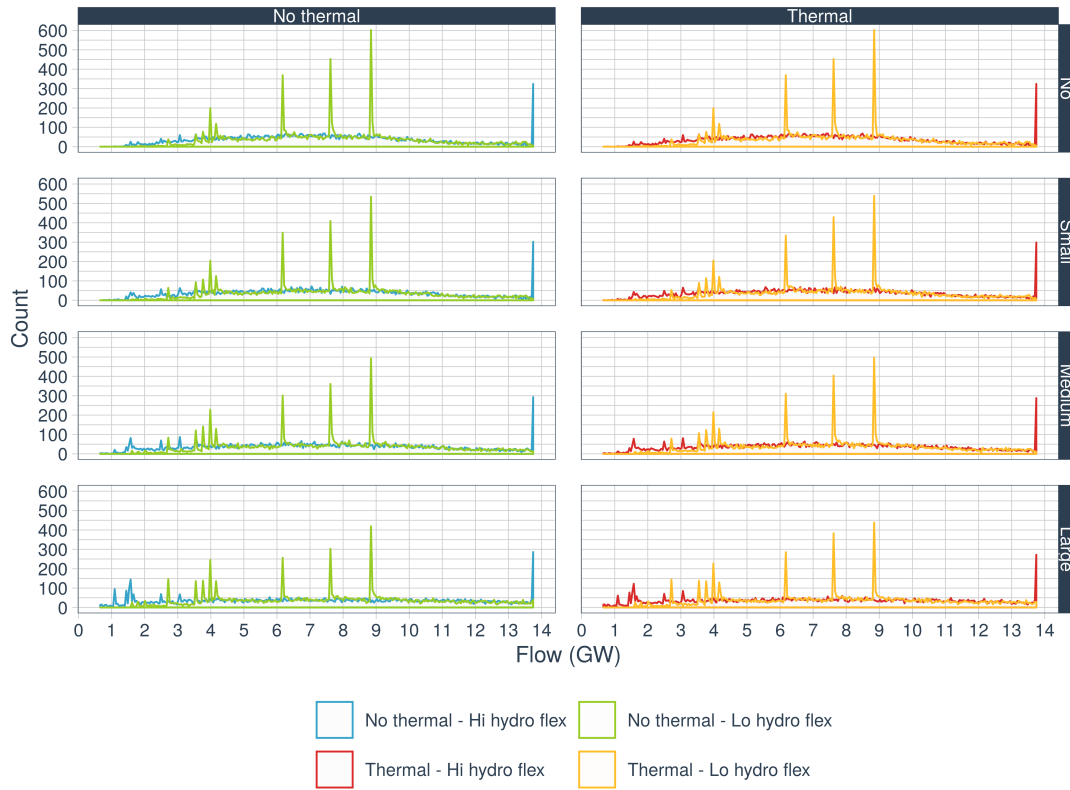


Figure A.13: Density plots of hourly hydro flows over for all scenarios. Panels left NO THERMAL and right THERMAL, from top to bottom: electrolyzer capacity.